

## Construction of transferable spherically averaged electron potentials

This article has been downloaded from IOPscience. Please scroll down to see the full text article.

1994 J. Phys.: Condens. Matter 6 5415

(<http://iopscience.iop.org/0953-8984/6/28/016>)

View [the table of contents for this issue](#), or go to the [journal homepage](#) for more

Download details:

IP Address: 171.66.16.147

The article was downloaded on 12/05/2010 at 18:53

Please note that [terms and conditions apply](#).

## Construction of transferable spherically averaged electron potentials

K Stokbro†, N Chetty‡, K W Jacobsen† and J K Nørskov†

† Centre for Atomic-scale Materials Physics and Physics Department, Technical University of Denmark, DK 2800 Lyngby, Denmark

‡ Department of Physics, Brookhaven National Laboratory, Upton, NY 11973, USA

Received 4 March 1994, in final form 20 April 1994

**Abstract.** A new scheme for constructing approximate effective electron potentials within density-functional theory is proposed. The scheme consists of calculating the effective potential for a series of reference systems, and then using these potentials to construct the potential of a general system. To make contact with the reference system the neutral-sphere radius of each atom is used. The scheme can simplify calculations with partial wave methods in the atomic-sphere or muffin-tin approximation, since potential parameters can be precalculated and then for a general system obtained through simple interpolation formulas. We have applied the scheme to construct electron potentials of phonons, surfaces, and different crystal structures of silicon and aluminium atoms, and found excellent agreement with the self-consistent effective potential. By using an approximate total electron density obtained from a superposition of atom-based densities, the energy zero of the corresponding effective potential can be found and the energy shifts in the mean potential between inequivalent atoms can therefore be directly estimated. This approach is shown to work well for surfaces and phonons of silicon.

One route that seems promising in order to construct computationally efficient *ab initio* schemes for calculating total energies and forces of solids is to exploit the variational properties of density-functional theory [1]. We have shown earlier how the total electron density can be decomposed into a superposition of transferable atom-based densities for metals and semiconductors [2, 3]. When such densities are used to generate an input density for the Harris functional [4, 5], excellent total energies are obtained for surfaces, phonons and structural differences [6, 3] due to the fact that the Harris functional is stationary in the density. In this way the self-consistency loop is avoided. It is the purpose of the present report to show how the variational nature of density-functional theory can be exploited even further by working with both approximate densities and potentials simultaneously.

The Hohenberg–Kohn density functional can be generalized to a functional  $E[n, v]$  which depends on both the density  $n$  and the potential  $v$  [5, 7] and which is stationary with respect to independent variations of the density and the potential. The general functional can be written

$$E[n, v] = \sum_{\alpha} \epsilon_{\alpha}[v] - \int n(\mathbf{r})v(\mathbf{r}) \, d\mathbf{r} + E_{e1}[n] + E_{xc}[n] \quad (1)$$

where  $\epsilon_{\alpha}$  denotes the eigenvalues generated by the potential  $v$ , and where  $E_{e1}[n]$  and  $E_{xc}[n]$  are the electrostatic and exchange–correlation energy functionals, respectively. If the potential is restricted to be a functional of the density, the Hohenberg–Kohn functional or the Harris functional appear as special cases [7]. The stationarity property of the general

functional with respect to variations in the potential can be utilized to construct efficient schemes for evaluation of total energies and Hellman–Feynman forces [3]. In the following we shall describe one such scheme which has its root in the effective-medium theory [7]. The scheme applies to situations in which the kinetic energy can be calculated within the muffin-tin or atomic-sphere approximation (ASA) with spherically symmetric potentials within the atomic spheres. The idea is to use self-consistently calculated potentials from a series of reference systems which we choose here to be a bulk crystal with varying lattice constant. For a given atom in a general system the potential within the atomic sphere around the atom is then approximated by the potential in the reference system with an appropriate lattice constant. The lattice constant of the associated reference system is determined by the requirement that a neutral sphere around the atom should have the same radius in the system under study and in the reference system.

The neutral sphere is a sphere containing three (four) electrons in the case of aluminium (silicon) in the pseudo-potential scheme. If the approach described here is combined with the density construction of [2] where the total electron density,  $n(\mathbf{r})$ , is approximated by a superposition of atom-based densities,  $\Delta n_{\text{atom}}$ , positioned at each atomic site,  $\mathbf{R}_i$ ,

$$n(\mathbf{r}) = \sum_i \Delta n_{\text{atom}}(|\mathbf{r} - \mathbf{R}_i|) \quad (2)$$

then the NS radius can be obtained directly, or simple interpolation formulas can be made from which the NS radius can be obtained with high accuracy [6, 3].

We have used this scheme to calculate the effective potential of silicon and aluminium atoms in different configurations. For silicon we use the diamond structure and for aluminium the FCC structure as reference systems. The lattice parameter is regarded as a parameter which can be varied in order to find a good approximation for the potential. To calculate the effective potentials we use a self-consistent plane-wave pseudo-potential program, with a 12 Rydberg cut-off for the plane-wave basis set. With this cut-off, we find the lowest-energy configuration of silicon to be the diamond lattice with lattice constant  $10.17 a_0$ , and for aluminium the FCC lattice with lattice constant  $7.48 a_0$ .

As test systems for silicon we consider the diamond longitudinal phonon at the X point (denoted LAO(X) and frozen at the displacement 0.02 in units of the lattice constant), the diamond (100) surface, and the FCC structure with a lattice constant of  $7.18 a_0$ . Similarly, for aluminium, we use the FCC longitudinal phonon at the X point (denoted L(X) and displacement 0.02), the FCC (100) surface, and the diamond structure with a lattice constant of  $11.05 a_0$ . These six structures cover the two elements in quite different surroundings, and if the potential construction works for these situations a high degree of transferability is guaranteed.

As the first test system, we consider silicon in the FCC structure. As noted in the introduction the way we make contact between the test system and the reference system is through the NS radius. In the FCC structure the NS radius is almost equal to the Wigner–Seitz (WS) radius, while the NS radius is substantially smaller than the WS radius in the diamond structure. This difference is due to the large regions in the diamond lattice which contain almost no charge and therefore are not included in the neutral sphere. In figure 1 we show the local part of the self-consistent effective potential of the FCC test system compared to that of the reference system with the same NS and WS radius as the FCC test system, respectively. Clearly the potential of the reference system chosen according to the NS criterion gives by far the best approximation to the FCC potential.

In order to quantify the difference in the potentials, we introduce the RMS error  $\sigma$ ,

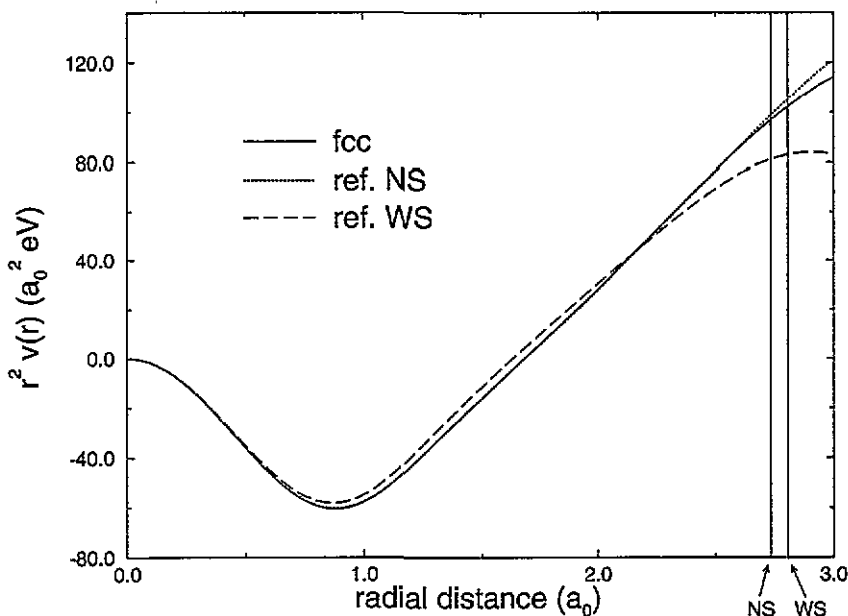


Figure 1. The figure shows the self-consistent effective potential (i.e.  $r^2 v(r)$ ) of silicon in the FCC structure (solid line) and that of the diamond reference system with the same NS radius (dotted line) and WS radius (dashed line), as a function of the radial distance. The potentials have been aligned such that the mean potential within the WS sphere is zero. The two vertical lines show the NS and WS radius of the FCC system, respectively.

defined by

$$\sigma^2 = \frac{3}{s_W^3} \int_0^{s_W} [\bar{v}(r) - \bar{v}^{\text{ref}}(r)]^2 r^2 dr \quad (3)$$

where  $s_W$  is the WS radius of the test system, and the two potentials are aligned such that they have the same average within the sphere. To get an estimate of the error in the potentials due to the finite plane-wave basis set, we have compared one of the reference potentials of silicon with that of an 18 Rydberg calculation. We find a RMS error of  $\sigma = 0.06$  eV, so this is the level of accuracy we ideally can obtain.

In figure 2 we show the RMS error between the potential of the FCC test system and the diamond reference system as a function of the WS radius (i.e. as a function of lattice constant) of the diamond lattice. We see that optimally the reference system should be chosen with a WS radius of  $3.18 a_0$ . We note that this is not at all close to the WS radius in the FCC test system ( $s_W = 2.806 a_0$ ). In the ASA the reference diamond structure is often embedded in a BCC structure with twice the number of spheres where only half of them contain an atom, and the others are empty. For this construction the sphere radius is a factor  $2^{1/3}$  smaller than the WS radius, and the reference system where this smaller sphere equals the FCC WS radius is given by  $s_W = 3.53 a_0$ , which still is far from the optimal reference system. However, the reference diamond lattice with the same NS radius as the FCC test system has a WS radius of  $3.178 a_0$ , and is therefore almost exact in the optimal reference system. This is not just a coincidence, since for all test systems investigated we have found this to be the case.

In table 1 we show the minimal RMS error between the potential of the six test systems

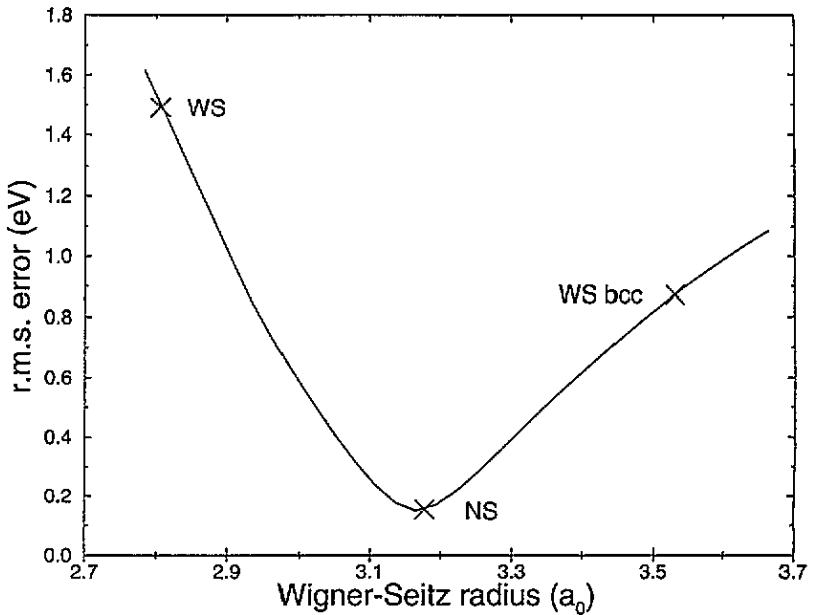


**Figure 2.** The figure shows the RMS error (equation (2)) between the effective potential of silicon in the FCC structure and the potential in the diamond reference system as a function of the WS radius of the reference system. The three crosses show the error when the reference system has the same WS radius, NS radius and BCC WS radius (diamond with empty spheres) as the FCC system, respectively.

**Table 1.** Calculated LMTO potential parameters for the three pseudopotentials of figure 1. For each angular component the appropriate non-local contribution to the potential has been added.

Potential	$C_p - C_s$ (eV)	$\Delta_s$ (eV)	$\Delta_p$ (eV)
SC FCC	10.968	1.566	1.358
Ref. NS	10.961	1.565	1.355
Ref. WS	10.998	1.703	1.475

and the reference system, compared to the error when the reference system is chosen to have the same NS radius or the same WS radius as the test system. It is evident from the table that using the reference potential chosen according to the NS criterion is almost optimal, while the WS criterion is far from optimal. It should be noted that if the integral in equation (2) were done within the neutral sphere instead of within the WS sphere, the NS criterion would give even smaller errors.

In order to estimate how much the errors induced by the approximations for the potential will affect the total energy, we show in table 2 the value of LMTO potential parameters [8] for the three potentials of figure 1. The potential parameters are calculated by solving the radial Schrödinger equation at a fixed energy for the s and p angular component ( $\epsilon_v = \{13.22, 18.96\}$ ), with the energy chosen at the centre of gravity of the occupied part of the FCC band. The accuracy of the potential parameters directly reflects the accuracy of the corresponding one-electron bands, and thereby the one-electron band energy. As seen from table 2 the potential parameters obtained with the NS criterion are in excellent

agreement with the self-consistent parameters, while the potential parameters obtained with the WS criterion are more than 10% off.

**Table 2.** The first row shows the minimal RMS error between the potentials of the six test systems and the reference system. The second and third row show the RMS error when the reference system is that with the same NS and WS radius as the test system, respectively. The first three columns show the errors for the three silicon test systems; the FCC structure, the (100) diamond surface and the diamond longitudinal phonon at the X point (LAO(X)) with a displacement of 0.02 in units of the lattice constant. The last three columns show the errors for the three aluminium test systems; the diamond structure, the FCC (100) surface and the FCC longitudinal phonon at the X point (L(X)) with displacement 0.02 in units of the lattice constant.

	Silicon			Aluminium		
	FCC	(100)	LAO(X)	Diamond	(100)	L(X)
$\sigma^{\min}$ (eV)	0.15	0.08	0.06	0.11	0.05	0.028
$\sigma^{\text{NS}}$ (eV)	0.15	0.20	0.08	0.24	0.10	0.034
$\sigma^{\text{WS}}$ (eV)	1.49	1.22	0.34	0.89	0.48	0.042

Until now we have aligned the average potentials within the WS sphere. However, for a surface calculation the mean potential at the surface is shifted relative to the bulk and we need to describe this shift in order to get a good estimate of the overall potential. At first sight the problem seems hard to overcome since the mean potential is arbitrary for a bulk calculation due to the divergence of the electrostatic potential [9]. However, it is possible to circumvent this problem if we use the potential constructed from a superposition of atom-based densities. We will name this potential the Harris potential since this is the effective potential used in the Harris functional, when the input density is obtained from a superposition of atom-based densities. We know from previous studies that when this potential is used as an input to the Harris functional, excellent total energies are obtained for phonons, surfaces, and different crystal structures [2, 6].

The electrostatic part of the Harris potential  $V_{\text{el}}^{\text{Harris}}$  can in a natural way be divided into a sum over atom-based electrostatic potentials  $v_{\text{el}}(r)$  each given by the sum of one ionic potential  $v_{\text{ion}}$  and the Hartree potential derived from one atom-based density  $\Delta n_{\text{atom}}$

$$V_{\text{el}}(r) = \sum_i v_{\text{el}}(|r - R_i|) = \sum_i \left( v_{\text{ion}}(|r - R_i|) + \int \frac{\Delta n_{\text{atom}}(|r' - R_i|)}{|r - r'|} dr' \right). \quad (4)$$

With this construction the  $1/r$  divergence of the electrostatic potential is avoided, since the atom-based density decreases exponentially, and thereby fixes the vacuum level. Note that a consequence of this is that within this approximation all surfaces of a solid will have the same work function. In contrast to the total energy the work function is not variational in the density, and we cannot expect the density *ansatz* equation (3) to produce an accurate estimate.

Having established a common energy zero for all Harris potentials we can now proceed to determine the energy shifts of the mean potential for atoms in different environments. In figure 3 the solid curve indicates the mean Harris potential for silicon in the reference diamond structure as a function of the NS radius. Also shown are the actual shifts of both the Harris and the self-consistent potential at the three principal surfaces and the potential shifts of the two inequivalent atoms in the LAO(X) phonon. These potential shifts are marked in the figure at the calculated NS radii of the atoms. We see that the potential shift in the reference system compares surprisingly well with the potential shifts in the test

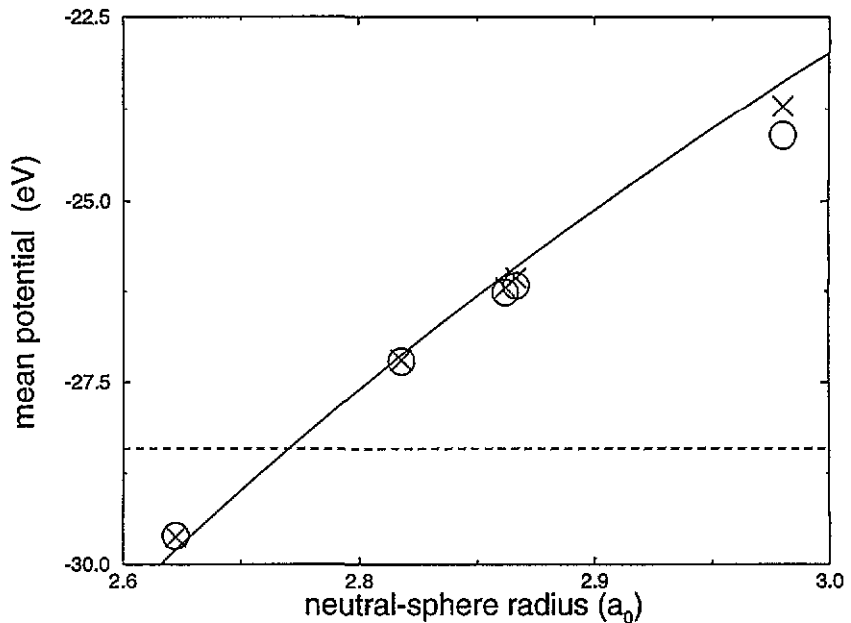


**Figure 3.** The solid curve shows the mean Harris potential, within the NS, of the diamond reference system as a function of the NS radius. The two first crosses show the shift in the mean Harris potential for the two inequivalent atoms in the LAO(X) phonon, at their NS radii. The last three crosses show the shift in the mean potential at the diamond (111), (110) and (100) surface, respectively. The circles show the shifts for the corresponding self-consistent potentials. The dotted line shows the mean potential in the equilibrium diamond lattice.

systems. On the average, the shift of the Harris potential is about 4% higher than for the self-consistent potential, and the shift of the reference system is about 8% higher than for the Harris potential.

**Table 3.** The RMS error of potential differences (equation (2)) for a silicon atom at the (100) surface. The differences are between the self-consistent surface potential  $V^{SC}$ , the Harris potential  $V^{Harris}$  for the surface with the density construction equation (3) and the analogous potentials in the diamond reference system chosen according to the neutral sphere (NS) criterion.

	$V^{SC} - V^{Harris}$	$V^{SC} - V_{ref}^{SC}$	$V^{SC} - V_{ref}^{Harris}$
$\sigma^{NS}$ (eV)	0.24	0.20	0.30

In table 3 we show the RMS error between the Harris potential and the self-consistent potential for a silicon atom at the diamond (100) surface. This is compared to the RMS error between the self-consistent surface potential and both the self-consistent and Harris potential of the reference system when the reference system is chosen according to the NS criterion. As seen from the table the RMS errors are similar for the three potentials, and since the total energies obtained using the Harris potential are excellent [6, 3], all three reference potentials are accurate enough to be used to calculate total energies.

In summary we have presented a scheme for obtaining transferable ASA potentials. The scheme was applied to six test systems consisting of silicon or aluminium atoms. The potentials obtained were in very good agreement with the actual self-consistent potentials,

reproducing both the radial variations and the shifts in the mean potential, and when used as input to the LMTO method accurate potential parameters were obtained. We expect the method to be valuable for constructing new approximate total energy schemes, and it is currently used in a new formulation of an effective-medium tight-binding model for silicon [3].

### Acknowledgments

We are grateful to H Skriver whose LMTO programs we have used for calculating the LMTO potential parameters. We would also like to thank K Kunc, O H Nielsen, R J Needs and R M Martin whose solid state programs we have used, and E L Shirley who developed the pseudo-potential routines. This work was in part supported by the Danish Research Councils through the Centre for Surface Reactivity. The Centre for Atomic-scale Materials Physics is sponsored by the Danish National Research Foundation. Nithaya Chetty acknowledges support from the Division of Materials Sciences, US Department of Energy under contract No DE-AC02-76CH00016.

### References

- [1] Hohenberg P and Kohn W 1964 *Phys. Rev.* **136** 3864  
Kohn W and Sham L J 1965 *Phys. Rev.* **140** A1133
- [2] Chetty N, Jacobsen K W and Nørskov J K 1991 *J. Phys.: Condens. Matter* **3** 5437
- [3] Stokbro K, Chetty N, Jacobsen K W and Nørskov J K 1994 to be published
- [4] Harris J 1985 *Phys. Rev. B* **31** 1770
- [5] Foulkes W M C and Haydock R 1989 *Phys. Rev. B* **39** 12520
- [6] Chetty N, Stokbro K, Jacobsen K W and Nørskov J K 1992 *Phys. Rev. B* **46** 3798.  
Stokbro K, Chetty N, Jacobsen K W and Nørskov J K 1993 *Proc. 15th Tanigushi Symp.* (Berlin: Springer)
- [7] Jacobsen K W, Nørskov J K and Puska M J 1987 *Phys. Rev. B* **35** 7423
- [8] Andersen O K, Jepsen O and Sob M 1987 *Electronic Bandstructure and its Applications (Springer Lecture Notes 1987)* ed M Yussouff (Berlin: Springer)  
Skriver H L 1984 *Muffin Tin Orbitals and Electronic Structure* (Berlin: Springer)
- [9] Kleinman L 1981 *Phys. Rev. B* **24** 7412